Polydopamine coating on a thin film composite forward osmosis membrane for enhanced mass transport and antifouling performance

Hao Guo [a], Zhikan Yao [a], Jianqiang Wang [a], Zhe Yang [a], Xiaohua Ma [a,b], Chuyang Y. Tang [a *]

[a] Department of Civil Engineering, The University of Hong Kong, Pokfulam, Hong Kong

[b] Shanghai Key Laboratory of Multiphase Materials Chemical Engineering, Chemical Engineering Research Center, East China University of Science and Technology, 130 Meilong Road, Shanghai 200237, PR China

*Corresponding Author:

Chuyang Y. Tang, tangc@hku.hk

Phone: +852 28591976

Fax: +852 25595337

Abstract

We applied a polydopamine (PDA) coating on a thin film composite (TFC) forward osmosis (FO) membrane and investigated the effects of coating on FO mass transport and antifouling behavior. The PDA coating significantly improved membrane surface hydrophilicity as well as reduced membrane surface roughness. Using a short PDA coating duration of 0.5 h, the coated membrane TFC-C0.5 achieved enhanced FO water flux and reduced reverse solute diffusion simultaneously. The reduced reverse solute diffusion can be attributed to the enhanced membrane selectivity: TFC-C0.5 had better rejection and similar water permeability compared to the original TFC membrane. This reduction in reverse solute diffusion further reduced the internal concentration polarization inside the coated membrane, leading to an enhanced FO water flux. Nevertheless, longer PDA coating duration of 1-4 h resulted in reduced FO water flux due to the significantly increased hydraulic resistance of the coated membranes. The PDA coated membrane TFC-C0.5 also presented an improved antifouling performance compared to the control membrane using alginate as a model foulant. Our results reveal the great room for the development of effective coating materials in FO: a well-designed coating with high selectivity and low hydraulic resistance can improve solute rejection, reduce reverse solute diffusion, mitigate internal concentration polarization and enhance FO water flux in addition to control fouling. Such unprecedented opportunities break the traditional trade-off between water flux and antifouling performance when coating pressure driven reverse osmosis membranes.

Keywords

Forward osmosis, polydopamine, coating, mass transport, antifouling

1. Introduction

Forward osmosis (FO) is a membrane process using a draw solution with high osmotic pressure to extract water from a feed solution with low osmotic pressure [1, 2]. In comparison with pressure-driven membrane processes such as reverse osmosis (RO) and nanofiltration (NF), FO requires lower energy input. This feature enables it being a potential alternative to address many water issues, such as seawater desalination [3, 4], wastewater treatment [5-7], and power generation (i.e., by pressure retarded osmosis) [8-10]. Despite the promising applications of FO, its performance can still be significantly limited by membrane fouling [11-14] and mass transport limitations [15, 16].

Surface modification is considered as a feasible approach for improving membrane antifouling performance [17-19]. One of the frequently used modification approaches is a mussel-inspired polydopamine (PDA) initiated coating [20-23]. PDA coating layer can be formed through the self-polymerization of dopamine on various substrates [24]. It can improve membrane surface hydrophilicity to reduce fouling [25, 26]. Therefore, PDA coating has been extensively investigated as an antifouling coating for pressure-driven membrane processes (e.g. RO, NF, and ultrafiltration) [20, 27, 28]. In recent years, PDA coating was also introduced on FO membranes to improve membrane performance. Arena et al. [29, 30] reported the use of PDA for improving the hydrophilicity of membrane support layers, which effectively reduced internal concentration polarization (ICP) and improved water flux . Han et al. [31] also reported that PDA-modified substrate layer can enhance membrane performance

in FO . Nevertheless, there is few study focusing on the use of surface coating (e.g. PDA coating) to modify the rejection layer of thin film composite (TFC) FO membranes. The transport phenomena (e.g. water transport and reverse solute diffusion) as well as the fouling behavior in the presence of a thin coating layer are still unknown in FO. Therefore, it is worthwhile to study the separation performance and antifouling behavior of a coated membrane and further elucidate the underlying mechanisms, since surface coating has been regarded as an important approach for enhancing membrane performance [17, 28, 32].

In this work, we applied a PDA coating on a commercial TFC FO membrane from Hydration Technology Innovations (HTI). Membrane separation performance and antifouling behavior were systematically investigated under various PDA coating conditions. The results will provide mechanistic understanding on the influence of surface coating on FO membrane performance, and may open new insight for the design of effective surface coating for FO membranes.

2. Materials and methods

2.1 Membranes and chemicals

The TFC FO membranes used in this study were provided by HTI (Albany, OR). This membrane consists of a polyamide rejection layer and a porous supporting layer embedded on a polyester mesh [33].

Unless specified otherwise, all the chemicals used in this study are analytical grade. Deionized (DI) water was used for the preparation of all solutions. Dopamine hydrochloride (J&K Scientific Ltd.) and tris (Acros Organics, Geel, Belgium) were used to form PDA coating layer. Sodium chloride (Uni-Chem) was used to prepare draw solution (DS) and feed solution (FS). Sodium hydroxide (Uni-Chem), and hydrochloride acid (37 wt%, VWR, Dorset, U.K.) were used to adjust solution chemistry. Sodium alginate and calcium chloride were supplied by Sigma-Aldrich (St. Louis, MO) and used in fouling experiments.

2.2 Preparation of PDA coating

The preparation of PDA coating has been described in details in our previous work [26]. Briefly, a clean membrane coupon was placed in a container with only the rejection layer exposed in the coating solution. A 150 mL solution containing 0.2 wt. % dopamine chloride and 10 mM tris at pH 8.5 was subsequently added to the container. The coating was performed under moderate shaking for a predetermined duration (0.5, 1, and 4 h). The coated membranes were denoted as TFC-C0.5, TFC-C1, and TFC-C4. All the coated membranes were thoroughly rinsed by DI water to remove unreacted residues before further testing.

2.3 Membrane characterization

A field-emission scanning electron microscope (FE-SEM, LEO 1530) was used to characterize membrane surface morphology. Dried membrane samples were sputter-coated with a thin layer of gold (BAL-TEC SCD 005). SEM was operated at an acceleration voltage

of 5.0 kV. An attenuated total reflectance Fourier transformation infrared spectrometer (ATR-FTIR, Perkin Elmer Spectrum 100) was employed to characterize membrane surface functional groups over a wavenumber range from 650 to 4000 cm^{-1}. An atomic force microscope (AFM, JPK Nano Wizard AFM) was used to resolve membrane surface roughness. A contact angle goniometer (OCA20, Dataphysics) was applied to determine water contact angles of membranes using a sessile drop method at 25℃. The reported value of contact angle is an average value of ten duplicates. A zeta potential analyzer (SurPASS, Anton Paar GmbH) was used to evaluate membrane surface charge with an adjustable gap cell and using 10 mM NaCl as background solution over a pH range from 3 to 10.

Membrane intrinsic properties including pure water permeability and solute permeability of the TFC FO membrane were evaluated in a pressurized RO mode using a lab-scale cross-flow filtration setup [26]. Briefly, a membrane coupon was placed in a filtration cell (CF042, Sterlitech) with an effective membrane area of 42 cm^2. A 10 L feed solution (i.e., DI water or 10 mM NaCl) was then recirculated for 12 h at 10 bar with a cross-flow velocity of 22.4 cm/s to pre-compact the membrane. Pure water permeability, *A*, and solute permeability, *B*, are determined by [34]

$$A = \frac{J_{v,RO}}{\Delta P - \Delta \pi} \quad (1)$$

$$B = \left(\frac{1}{R_{RO}} - 1\right) \times J_{v,RO} \quad (2)$$

where $J_{v,RO}$ ($Lm^{-2}h^{-1}$) is the water flux under RO mode, ΔP (bar) is the hydraulic pressure

difference across the membrane, $\Delta\pi$ is the osmotic pressure difference across the membrane, and R_{RO} is the solute rejection.

2.4 FO system

The FO membrane rejection tests and fouling experiments were conducted on a bench-scale cross-flow FO filtration system (Appendix A). An FO membrane coupon was placed in a cross-flow FO cell (CF042-FO, Sterlitech, effective membrane area of 42 cm^2). Diamond-patterned spacers were placed on the both sides to provide support for membrane and improve mass transfer [15, 34]. Two gear pumps were used to recirculate the feed solution (FS, of 1.5 L 10 mM NaCl) and draw solution (DS of 1.5 L NaCl over a concentration range of 0.5-2 M), respectively. The flow rates of both FS and DS were ~ 0.15 L/min. Water flux was determined at specific time intervals by measuring the weight of the feed tank with a digital balance connected to a data recording program. The conductivity of the feed solution was monitored with a benchtop conductivity meter. The salt rejection, R_{FO}, in FO was defined as [35]

$$R_{FO} = 1 - \frac{J_s}{J_v C_{fs}} \quad (3)$$

where J_s ($gm^{-2}h^{-1}$) is reverse solute flux, J_v ($Lm^{-2}h^{-1}$) is water flux in FO, and C_{fs} is the solute concentration in the feed solution. J_s/J_v is defined as the specific reverse solute diffusion. J_s was obtained as the slope of plotted $C_{fs,t}(V_{fs,0} - J_v A_m t)/A_m$ versus t, where $C_{fs,t}$ (gL^{-1}) is the solute concentration in FS at time t (h), $V_{fs,0}$ is the initial volume of FS (L), and A_m is the effective membrane area (m^2).

Fouling experiments were conducted with a FS containing 10 mM NaCl, 20 mg/L sodium alginate, and 1 mM $CaCl_2$. Prior to the fouling stage, FO membrane was pre-equilibrated with foulant-free FS and DS for 0.5 h. Subsequently, bulk alginate solution and calcium solution were spiked to the FS to reach the targeted concentration. The fouling experiment was then continued for 6 h.

3. Results and discussion

3.1 Membrane surface properties

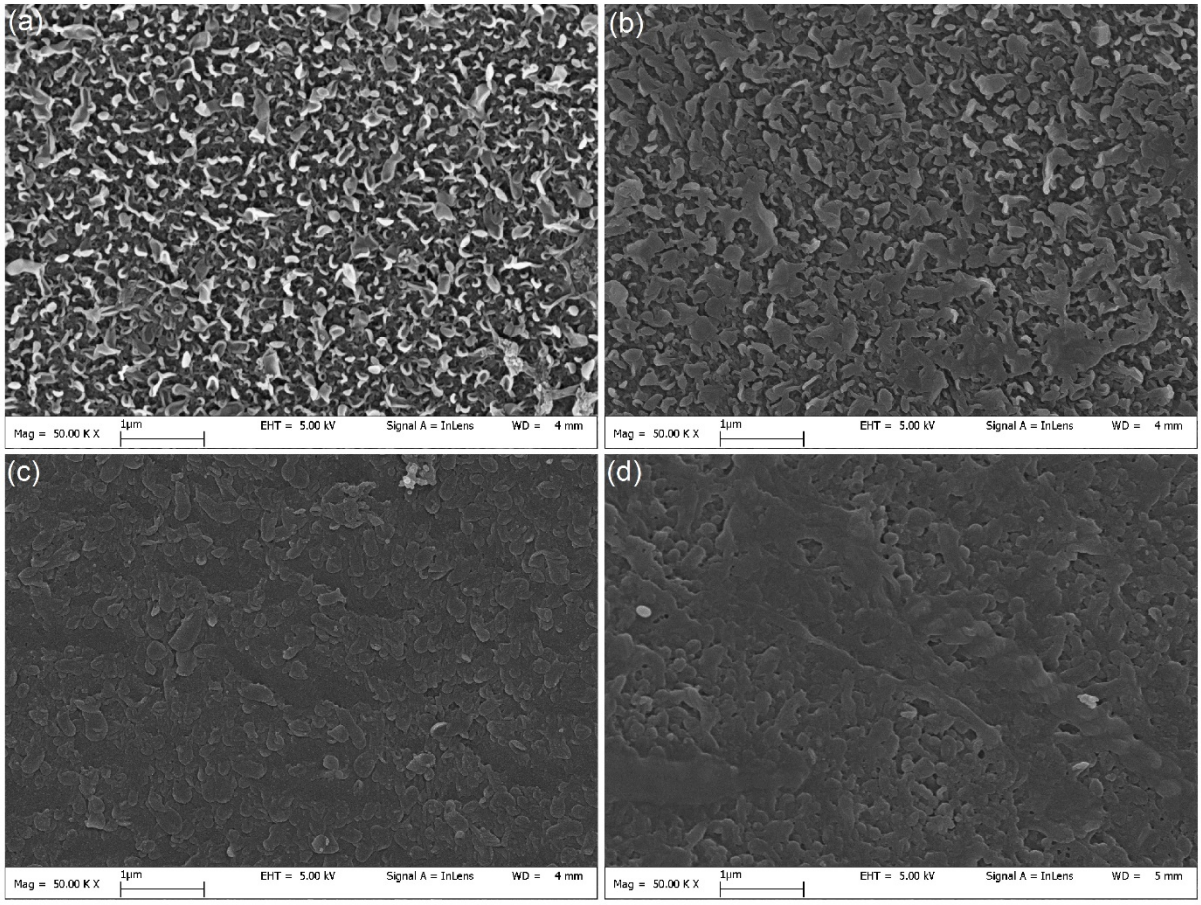

Figure 1. SEM images of the top surface layer of (a) control TFC, (b) TFC-C0.5, (c) TFC-C1, and (d) TFC-C4.

The surface morphology of various membranes were characterized by SEM (Figure 1). The control membrane shows an appearance of typical “ridge and valley” structure (Figure 1a), a characteristic of fully aromatic polyamide RO and NF membranes [36, 37]. The average roughness was ~48.9 nm (Figure 2a), which is comparable to the reported roughness of polyamide-based TFC membranes [26, 38]. The PDA coated membranes showed different morphology (Figure 1b-d) where the polyamide layer was partially or fully covered. Correspondingly, surface roughness also slightly reduced to 36.1 nm of TFC-C0.5, 41.6 nm of TFC-C1, and 42.3 nm of TFC-C4.

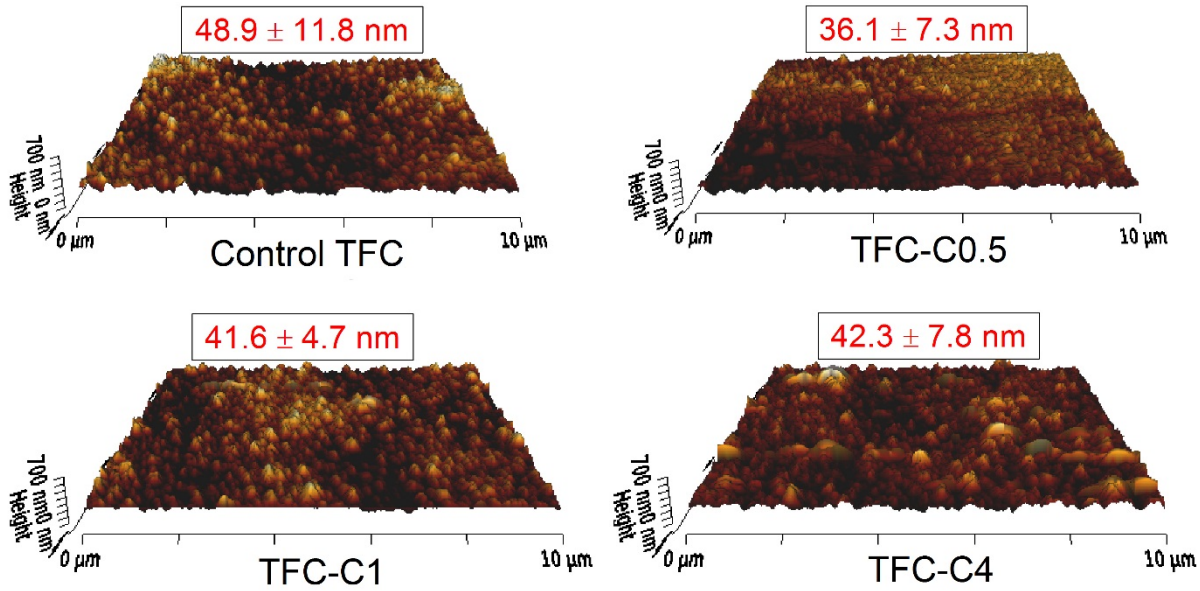

Figure 2. AFM images of the top surface layers of control and coated membranes. The scanned area are 10 µm × 10 µm.

Figure 3a presented the surface charge of control and coated membranes. There was no significant difference between the control membrane and TFC-C0.5 while TFC-C1 and TFC-C4 presented more negative surface. Water contact angles decreased significantly from

~42° of control membrane to ~25-29° of PDA coated membranes (Figure 3b), implying that the membrane surface became more hydrophilic with PDA coating. The improvement of hydrophilicity together with the decreased surface roughness might be beneficial to membrane antifouling [25].

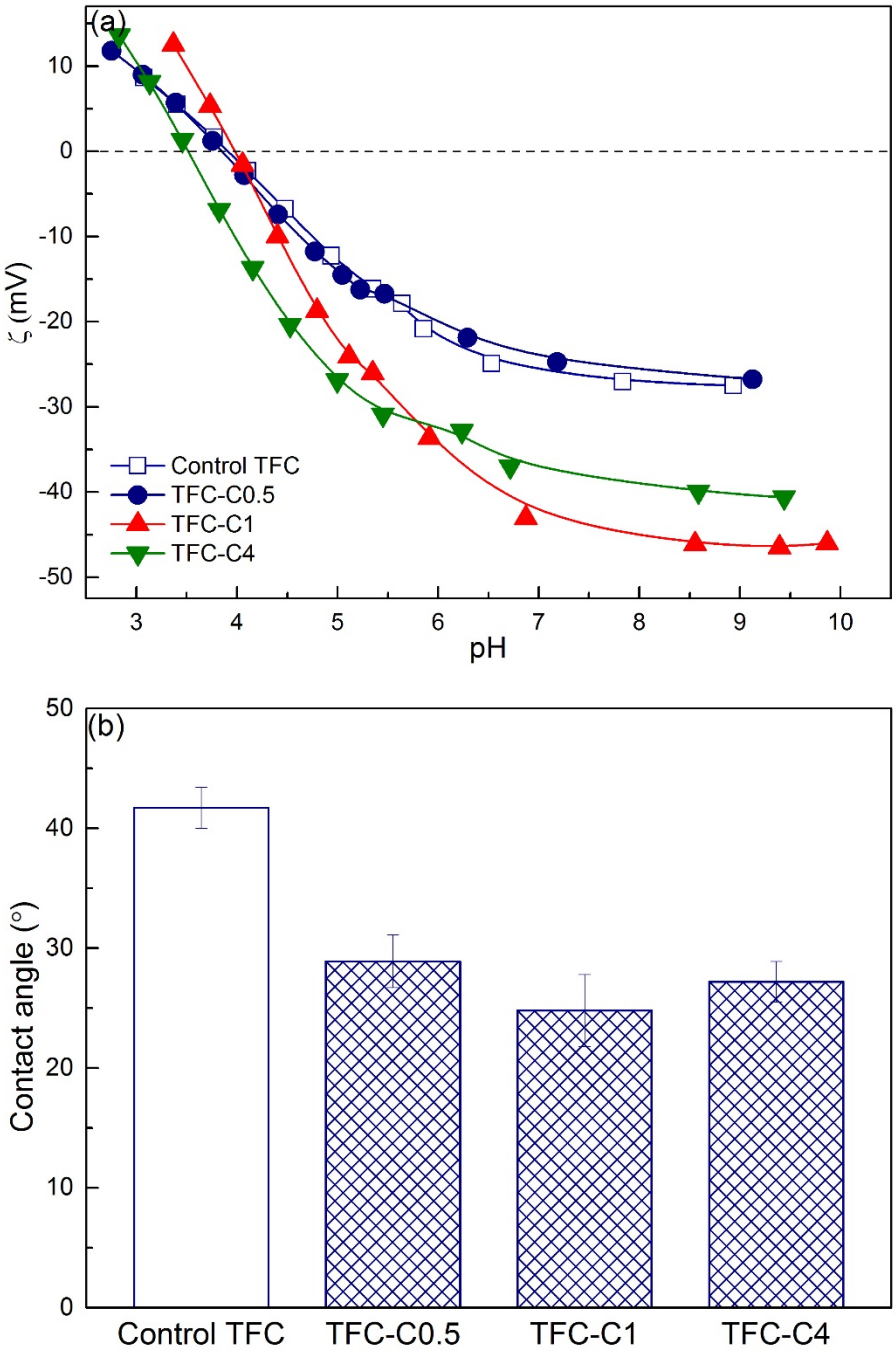

Figure 3. (a) Zeta potential of control TFC, TFC-C0.5, TFC-C1, and TFC-C4. The tests were performed in a background solution of 10 mM NaCl; (b) Water contact angles of control TFC, TFC-C0.5, TFC-C1, and TFC-C4.

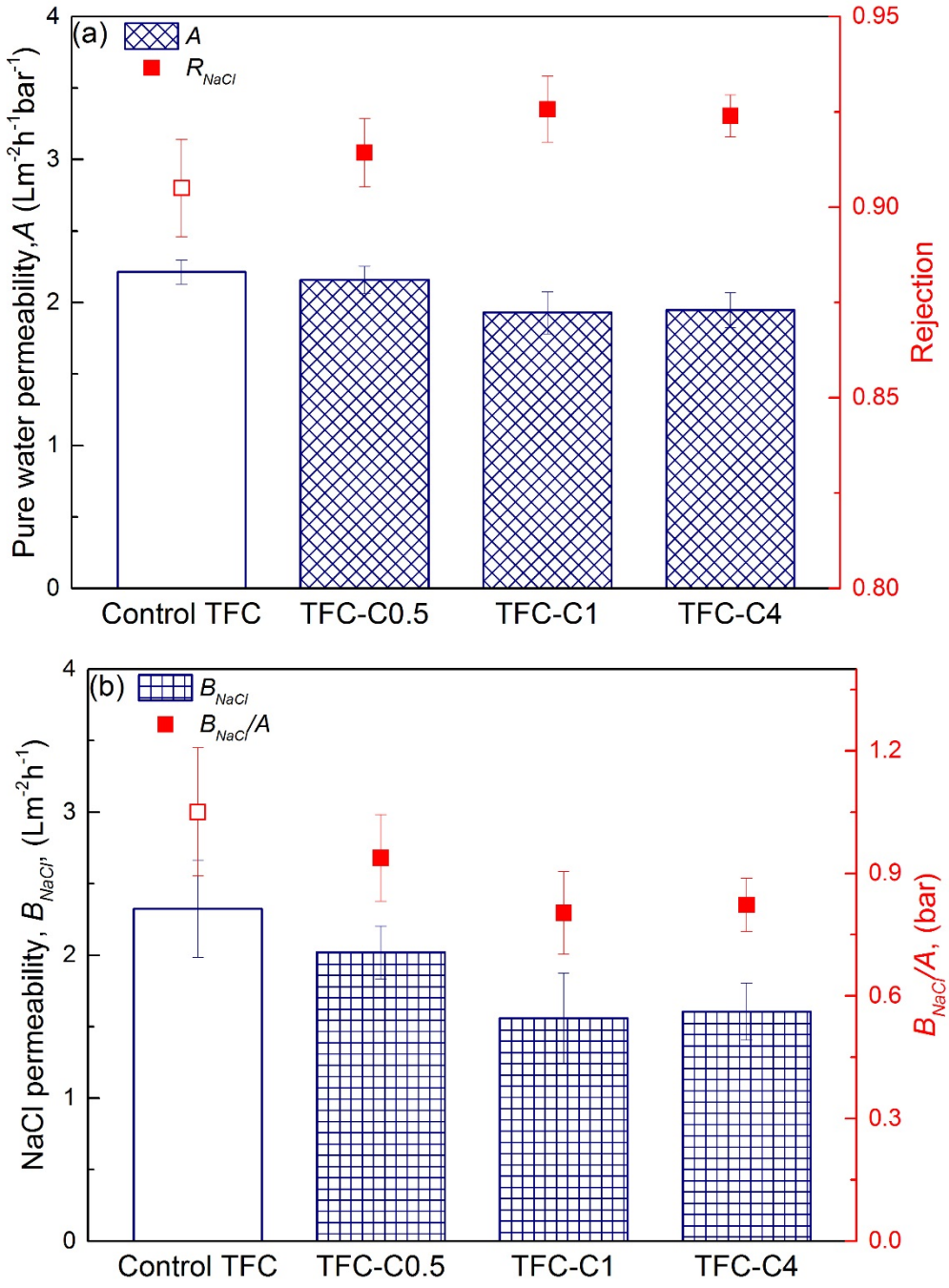

Figure 4. (a) Pure water permeability, *A*, and the rejection of NaCl, R_{NaCl}, (b) NaCl permeability, B_{NaCl}, and B_{NaCl}/A of various membranes. Test conditions: A, and R_{NaCl} were tested in the cross-flow RO setup with DI water and 10 mM NaCl as feed solution, respectively. The operating pressure was 10 bar.

193 3.2 Membrane separation properties

194 TFC-C0.5 with 0.5 h PDA coating presented a pure water permeability of ~2.2 $Lm^{-2}h^{-1}bar^{-1}$,
195 which is similar to that of control TFC membrane (Figure 4a). This result indicates that short
196 duration PDA coating (e.g., 0.5 h) only had marginal effect on water transport [32]. In
197 comparison, longer coating duration up to 4 h led to a reduced water permeability of ~ 1.9
198 $Lm^{-2}h^{-1}bar^{-1}$, which can be attributed to the increased resistance from the relatively thicker
199 PDA coating layer [20]. In general, the PDA coated membranes had improved salts rejection
200 (Appendix D). The permeability of NaCl decreased from ~2.3 $Lm^{-2}h^{-1}$ of control membrane to
201 ~1.6 $Lm^{-2}h^{-1}$ of TFC-C4 (Figure 4b), implying the enhanced membrane resistance to NaCl.
202 Furthermore, PDA coated membranes also presented decreased values of B_{NaCl}/A, an
203 important index of membrane selectivity [39, 40]. A decreased B_{NaCl}/A (i.e., enhanced
204 membrane selectivity to water against NaCl) is favored in FO because of its tendency to
205 reduce reverse solute diffusion [39].

206

207 3.3 FO performance

208 3.3.1 FO water flux and solute transport

209 The effects of PDA coating on FO water flux and reverse solute diffusion were evaluated in
210 AL-FS and AL-DS orientations (Figure 5). Both FO water flux and reverse solute diffusion
211 decreased upon longer PDA coating, as a result of the thicker coating layer [24]. As discussed
212 in *Section 3.1*, the PDA coating increased the resistance of the membrane to both water and
213 NaCl, which explains the overall decrease of FO water flux and reverse solute diffusion.

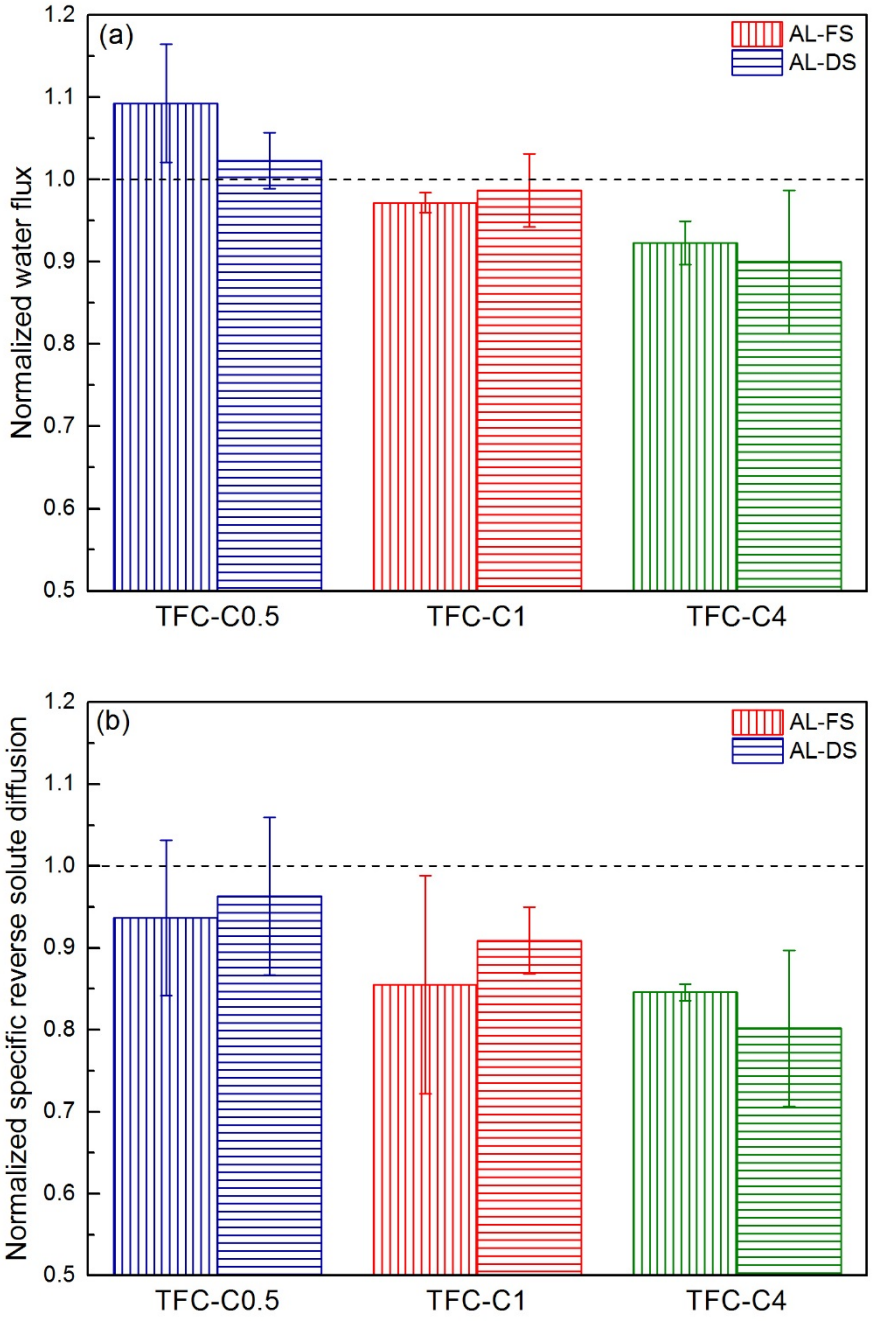

Figure 5. Effects of PDA coating on (a) water flux, and (b) specific reverse solute diffusion in both AL-FS and AL-DS orientations. The normalized value was calculated using the value of coated membrane divided by the correspondent value of control membrane (i.e., water flux of 9.0 ± 0.9 and 16.5 ± 1.1 $Lm^{-2}h^{-1}$, and specific reverse solute diffusion of 0.90 ± 0.24 and 0.82 ± 027 g/L for AL-FS and AL-DS, respectively). The dash line presents a normalized value of 1.0. Test condition: DS of 1 M NaCl, FS of 10 mM NaCl with pH of 6.5, equilibrium time of 0.5 h, running time of 1 h, and total time of 1.5 h.

Despite the overall decreased FO water flux, we observed that TFC-C0.5 had an improved

224 water flux compared to the base membrane (Figure 5a). Such peculiar results would not
225 usually occur for pressure driven RO membranes due to the additional hydraulic resistance
226 introduced by the coating. According to the resistance-in-series model [41], this additional
227 coating resistance decreased the net driving force (i.e., the hydraulic pressure difference)
228 across the rejection layer. In contrast, water flux of the concentration-driven FO process is
229 affected by ICP in addition to the membrane hydraulic resistance. In the current study, a short
230 PDA coating of 0.5 h enhanced membrane rejection, leading to reduced ICP as a result of
231 lower reverse solute diffusion ([42, 43] and Appendix G). The increased FO water flux upon
232 0.5 h PDA coating can thus be attributed to the dominance of ICP effect (reflected by the
233 reduced B_{NaCl}/A value) over the hydraulic resistance effect (reflected by similar A value).
234
235 The performance of TFC-C0.5 was also evaluated under DS concentration of 0.5, 1, and 2 M
236 NaCl (Figure 6). Systematical enhancement of water flux was observed at all tested DS
237 concentrations. At the meantime, reverse solute diffusion presented overall decrease in both
238 AL-FS and AL-DS orientations. The current study reveals the possibility of surface coating to
239 simultaneously improve FO water flux and rejection, which should be systematically
240 investigated in future study.

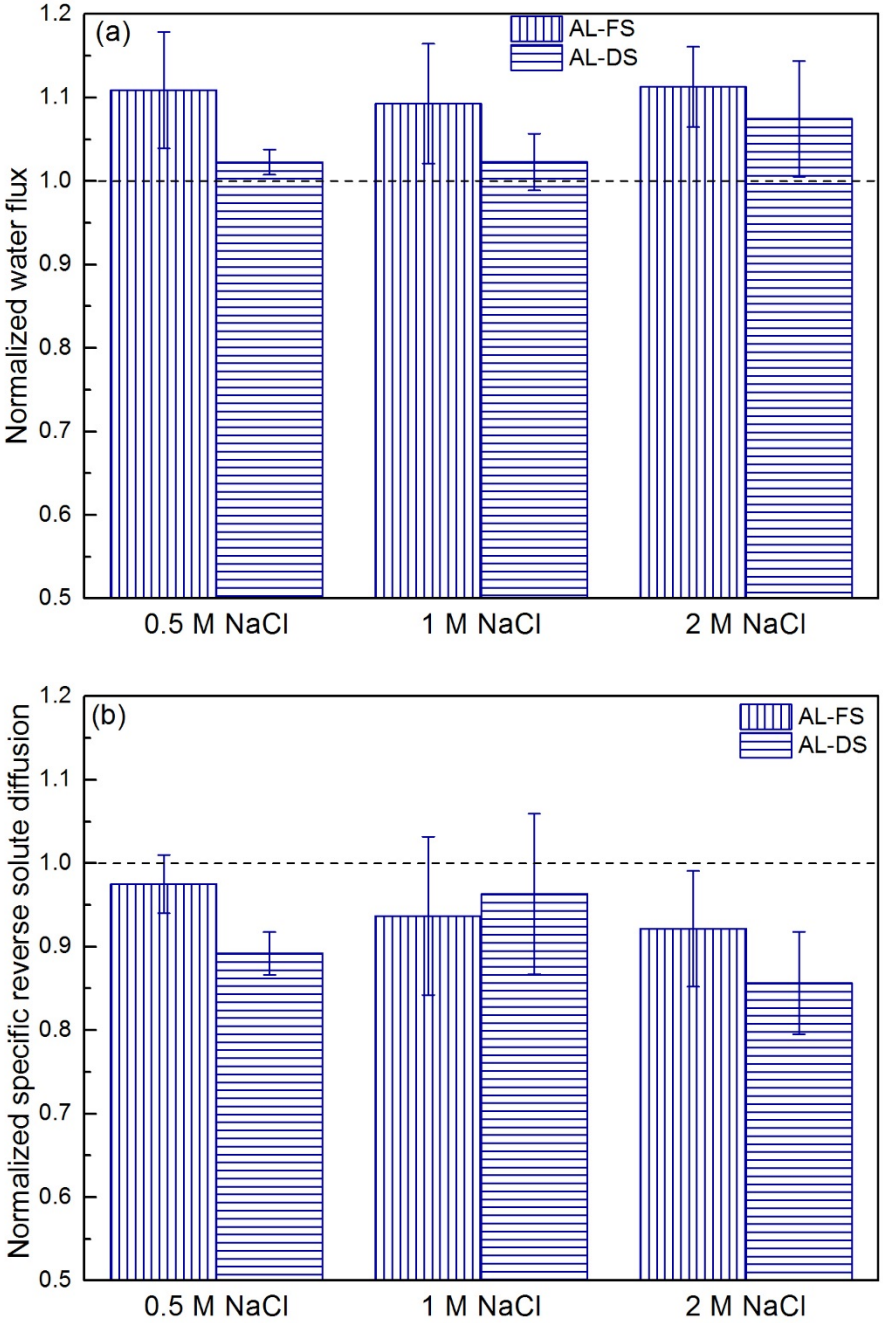

Figure 6. Effects of different DS concentration on (a) water flux and (b) specific reverse solute diffusion of TFC-C0.5 in both AL-FS and AL-DS orientations. The normalized value was calculated using the value of coated membrane divided by the correspondent value of control membrane (i.e., under AL-FS orientation, water flux of 6.0 ± 0.3, 9.0 ± 0.9, and 10.1 ± 0.5 $Lm^{-2}h^{-1}$, and specific reverse solute diffusion of 0.74 ± 0.10, 0.90 ± 0.24, and 0.78 ± 0.17 using 0.5, 1.0, and 2.0 M NaCl draw solutions, respectively; under AL-DS orientation, water flux of 11.3 ± 0.7, 16.5 ± 0.1.1, and 19.3 ± 2.3 $Lm^{-2}h^{-1}$, and specific reverse solute diffusion of 0.75 ± 0.07, 0.82 ± 0.27, and 0.98 ± 0.25 using 0.5, 1.0, and 2.0 M NaCl draw solutions, respectively). The dash line presents a normalized value of 1.0. Test condition: DS of 0.5-2 M NaCl, FS of 10 mM NaCl with pH of 6.5, equilibrium time of 0.5 h, running time of 1 h, and total time of 1.5 h.

252

253 3.3.2 FO fouling behavior

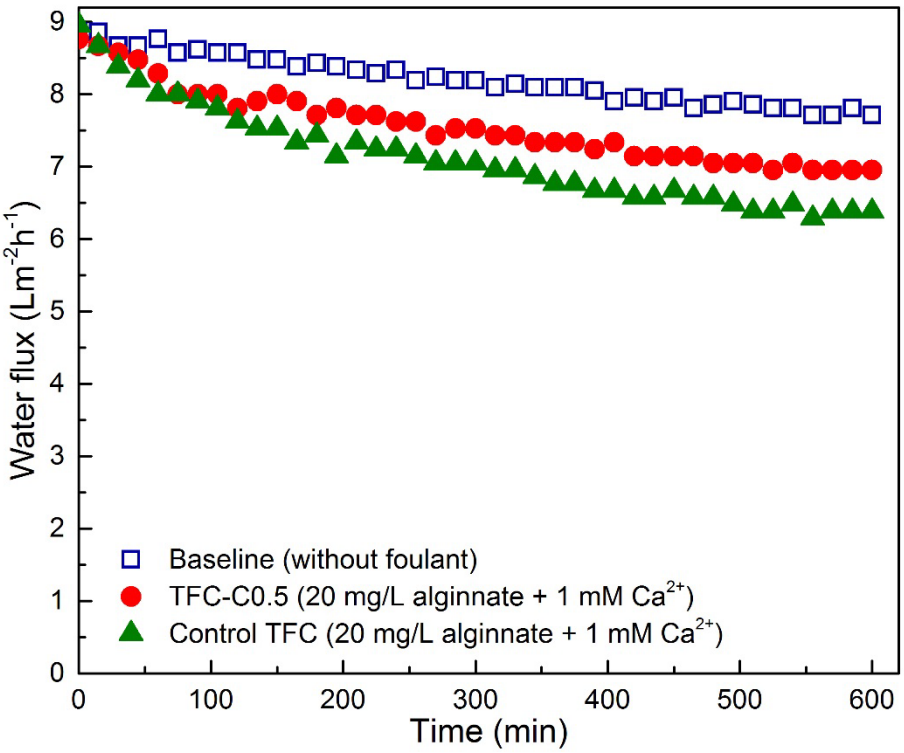

254

255 **Figure 7. Fouling behavior of control TFC and TFC-C0.5 in the orientation of AL-FS. Test conditions:**
256 **baseline experiment was conducted with 10 mM NaCl as FS and 1 M NaCl as DS; fouling**
257 **experiments were conducted with FS of 6.7 mM NaCl, 1 mM $CaCl_2$, and 20 mg/L alginate, and DS of**
258 **1 M NaCl. The running time of fouling experiments was 6 h.**

259

260 The fouling behavior of the control membrane and TFC-C0.5 are shown in Figure 7. The
261 initial flux of all tests was set to ~9 $Lm^{-2}h^{-1}$ by adjusting the DS concentration. The control
262 membrane experienced the greatest flux reduction. This membrane has a polyamide surface
263 chemistry whose carboxylic groups can have specific interactions with Ca^{2+} [37, 44]. The
264 calcium ions could form bridges between membrane surface and alginate, resulting in the
265 formation of alginate-calcium gel fouling layer and further decrease of water flux. In contrast,
266 TFC-C0.5 gave a better water flux behavior, confirming the antifouling effect of PDA coating

[45, 46]. The presence of thin PDA coating layer weakened the interfacial interaction between membrane surface carboxylic groups and Ca^{2+}, thus it restricted the formation of alginate-Ca gel network. In addition, a more hydrophilic and smoother surface of TFC-C0.5 may contribute to the antifouling performance because of reducing the adhesion of the gel on membrane surface [25]. A prior study [47] has also demonstrated the stability of PDA coating against membrane cleaning.

3.4 Implications

Membrane fouling has been a critical challenge for membrane-based wastewater reclamation [12, 48-50]. Surface modification is an effective way to enhance membrane resistance to fouling [17]. In current study, we investigated the use of PDA coating to enhance membrane antifouling performance in FO. A short duration PDA coating significantly improved membrane antifouling property and enhanced membrane separation performance (e.g., increased water flux and decreased reverse solute diffusion). In the context of pressure driven RO/NF processes, membrane surface coating will generally lead to reduced water flux. As a result, there is a trade-off between enhancing antifouling versus compromised separation performance. However, the water transport in FO is not only affected by overall membrane resistance but also influenced by the membrane selectivity. A well-designed coating can thus enhance both separation performance (rejection and water flux) and antifouling.

Selectivity (i.e., B/A) is a critical parameter for the design of coatings for FO membranes [39,

40]. A high selectivity to water and against solute (i.e., low *B/A*) can be beneficial for reducing reverse solute diffusion without significantly sacrificing water flux in FO. As a result, it can thus reach an increased rejection of targeted compounds (e.g., heavy metals and trace contaminants in the feed solution), reduced reverse solute diffusion, lowered internal concentration polarization, and enhanced FO water flux in addition to improved antifouling performance. Therefore, it is worthwhile to explore additional coating materials such as zwitterionic coating [51, 52], carbon-based coating [53, 54], and functionalization methods [55, 56] in the future studies. At the meantime, systematical investigations on the effects of coating on the FO performance under various application conditions (e.g., wastewater reclamation vs. seawater desalination) are needed.

4. Conclusions

This study investigated the effects of PDA coating on the FO water flux, solute transport, and antifouling performance. The results indicated that PDA coating layer could significantly improve membrane surface hydrophilicity and reduce membrane surface roughness. Using a short PDA coating duration of 0.5 h, the coated membrane TFC-C0.5 presented a reduced NaCl permeability and similar water permeability compared with the control membrane. The improved selectivity enabled TFC-C0.5 to achieve a higher FO water flux together with reduced reverse solute diffusion under various DS concentrations (0.5-2 M NaCl) in both AL-FS and AL-DS orientations. The enhanced FO water flux of TFC-C0.5 can be attributed to the reduced internal concentration polarization as a result of the improved membrane

selection. Nevertheless, longer PDA coating duration led to reduced FO water flux due to the dominance of increased hydraulic resistance of the thicker coating. The PDA-coated membrane TFC-C0.5 showed a better antifouling performance during alginate fouling. For the first time, this study reveals the possibility of simultaneously enhancing FO water flux, solute rejection, and antifouling performance through the use of a highly selective coating layer.

Acknowledgements

The authors thank the support from the General Research Fund (Project number 17207514) by the Research Grants Council of Hong Kong. The partial support from Strategic Research Theme (Clean Energy) and the Seed Grant for Basic Research (201511159141) of the University of Hong Kong were also appreciated. HTI is thanked for providing membrane samples.

Appendix A. Laboratory forward osmosis (FO) filtration setup

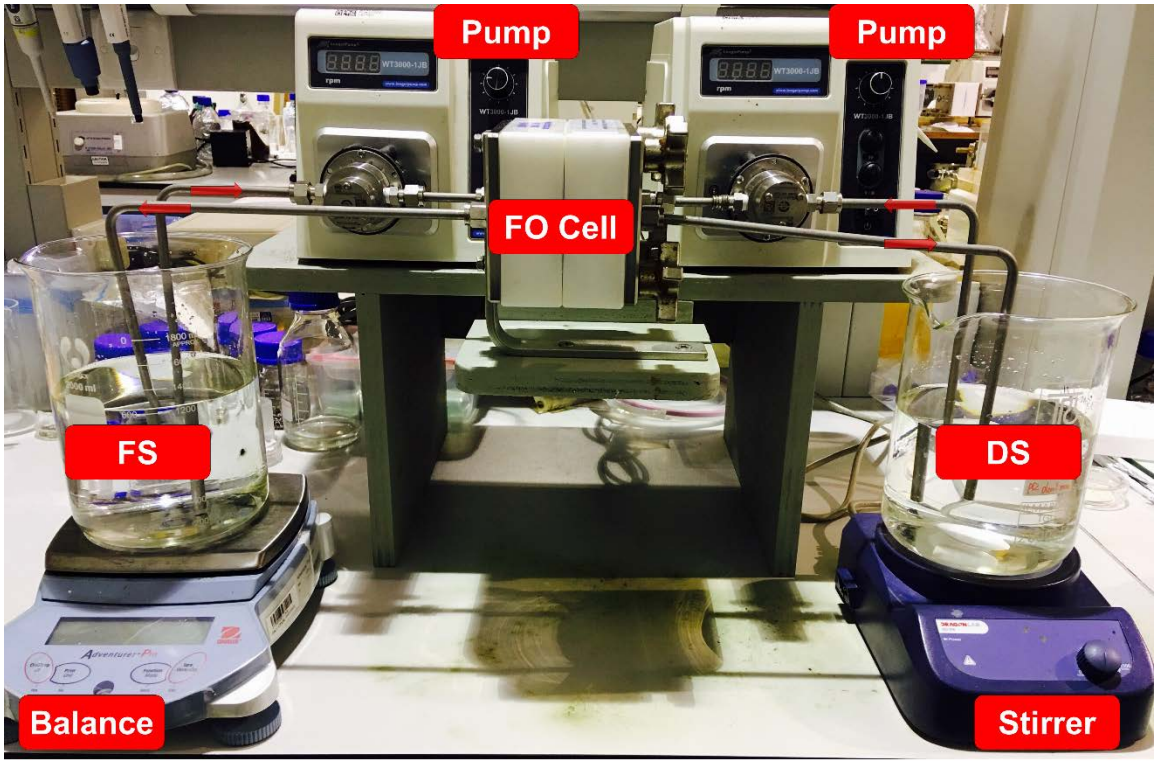

Figure A1. FO filtration setup used in this study.

Figure A1 presents the laboratory FO filtration setup in this study. An FO cell (CF042-FO, Sterlitech, effective membrane area of 42 cm^2) was used. Two gear pumps were used for the recirculation of draw solution (DS) and feed solution (FS), respectively. The mass and conductivity of FS were monitored by a digital balance and a conductivity meter (not shown in the picture), respectively.

Appendix B. Cross section SEM images of the control TFC and TFC-C4

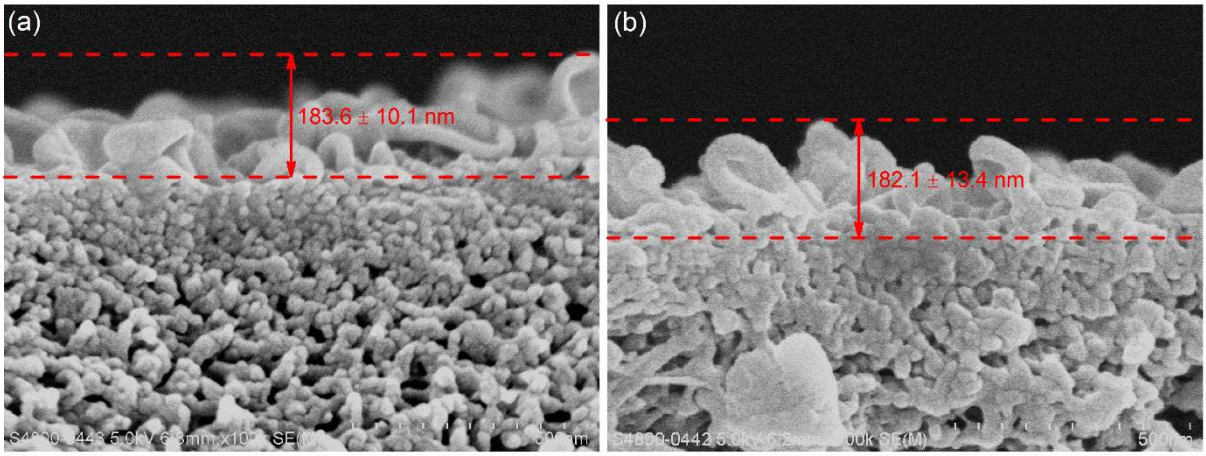

Figure B1. Cross section SEM images of (a) the control TFC and (b) TFC-C4.

The SEM cross-sectional images of the control TFC and TFC-C4 are presented in Figure B1. It was difficult to obverse the PDA coating for TFC-4 since its thickness was an order of magnitude (estimated to be ~ 20 nm with a growth rate of ~ 5 nm/h [24]) smaller than the roughness features of the membrane (nearly 200 nm).

Appendix C. FTIR-ATR spectrum of virgin and coated TFC membranes

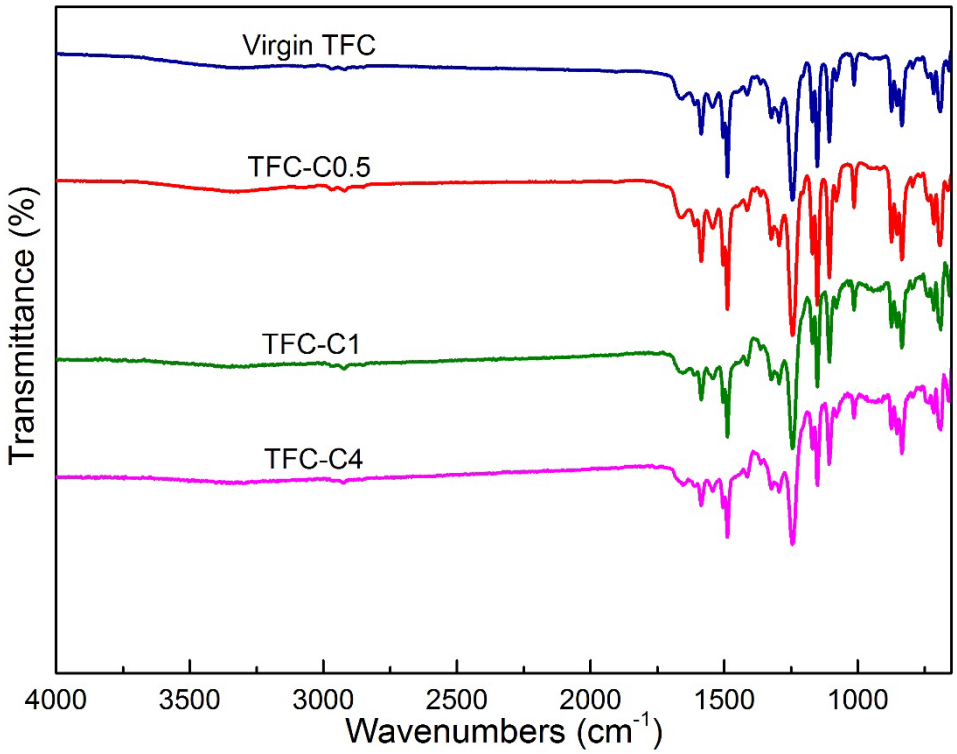

Figure C1. FTIR-ATR spectrum of virgin TFC, TFC-C0.5, TFC-C1, and TFC-C4 over a wavenumber range from 650 to 4000 cm^{-1}.

No significant peak shifting was observed in FTIR-ATR spectrum (Figure C1), in consistence with previous studies of coating PDA on polyamide membranes [26, 30], as a result of the ultrathin coating thickness (approximately 5 nm/h [24]) and the overlapping characteristic peaks of PDA and polyamide.

Appendix D. The rejection of $CaCl_2$ for control and coated membranes

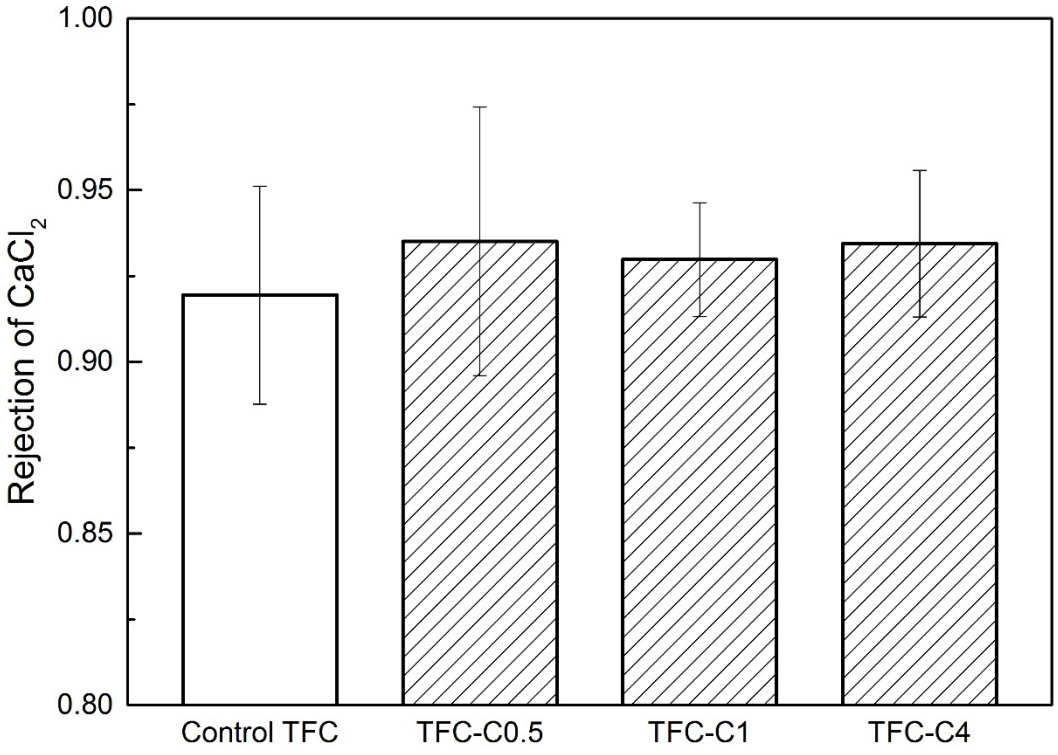

Figure D1. The rejection of $CaCl_2$ for control TFC, TFC-C0.5, TFC-C1, and TFC-C4. Test conditions: The rejection was tested in the cross-flow RO setup with 3.3 mM $CaCl_2$ as feed solution. The operating pressure was 10 bar.

The rejection of $CaCl_2$ for the control membrane and PDA coated membranes are shown in Figure D1. The PDA coating slightly increased the membrane rejection of $CaCl_2$.

Appendix E. The rejection of $CaCl_2$ for control and coated membranes

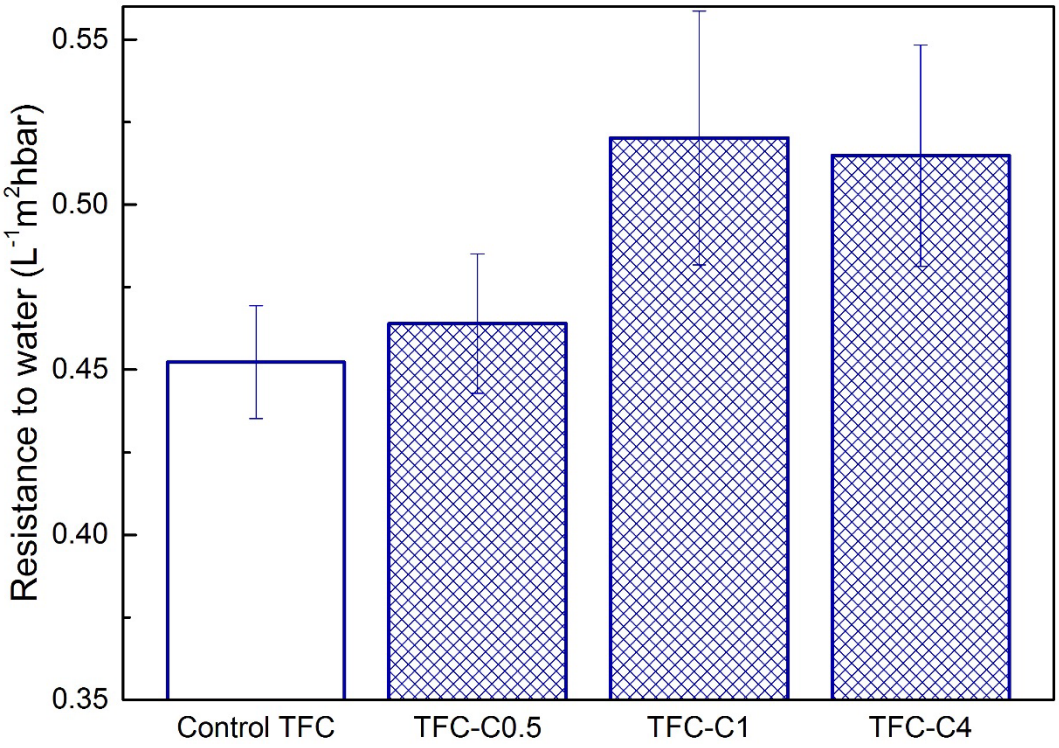

Figure E1. Membrane resistance to water, i.e., 1/A. The presented values were average values.

The water flux in FO can be affected by hydraulic resistance of the membrane and ICP (affected by reverse solute diffusion). A PDA coating layer improves membrane rejection (and thus reduces reverse solute diffusion) at the expense of increased membrane hydraulic resistance (Figure 4). Such trade-off relationship requires a careful optimization of the PDA coating duration. Despite that the 1 h PDA coated TFC-C1 presented slightly lower NaCl permeability B_{NaCl} and B_{NaCl}/A values than TFC-C0.5 (Figure 4), its hydraulic resistance was much greater (Figure E1). As a result, we found that TFC-C1presented lower FO water flux compared to TFC-C0.5 (Figure 5).

Appendix F. Comparison of FO water flux between TFC-C0.25 and TFC-C0.5

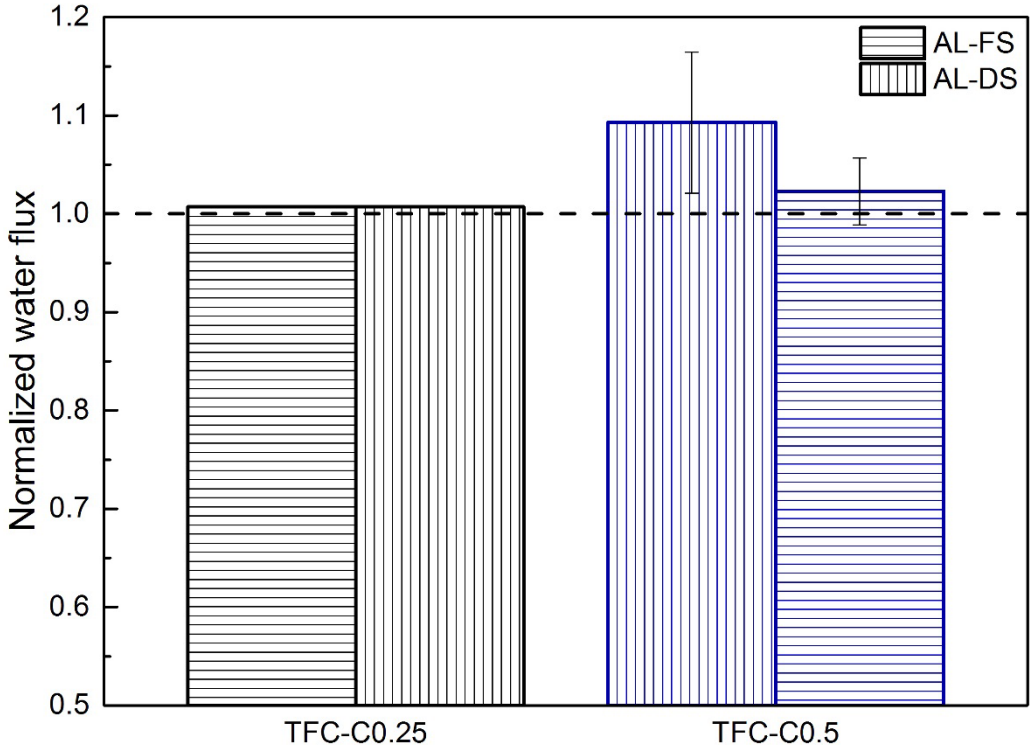

Figure F1. Normalized water flux in FO for TFC-C0.25 and TFC-C0.5. The normalized value was calculated using the value of coated membrane divided by the correspondent value of control membrane (i.e., water flux of 9.0 ± 0.9 and 16.5 ± 1.1 $Lm^{-2}h^{-1}$ for AL-FS and AL-DS, respectively). The dash line presents a normalized value of 1.0. Test condition: DS of 1 M NaCl, FS of 10 mM NaCl with pH of 6.5, equilibrium time of 0.5 h, running time of 1 h, and total time of 1.5 h.

A short time PDA coating duration of 15 min was applied on the TFC membrane (membrane denoted as TFC-C0.25). The result showed no significant change on FO water flux for TFC-C0.25 over the uncoated membrane (Figure F1). In comparison, TFC-C0.5 with 30 min coating had improved FO water flux.

Appendix G. Effect of membrane selectivity on FO water flux

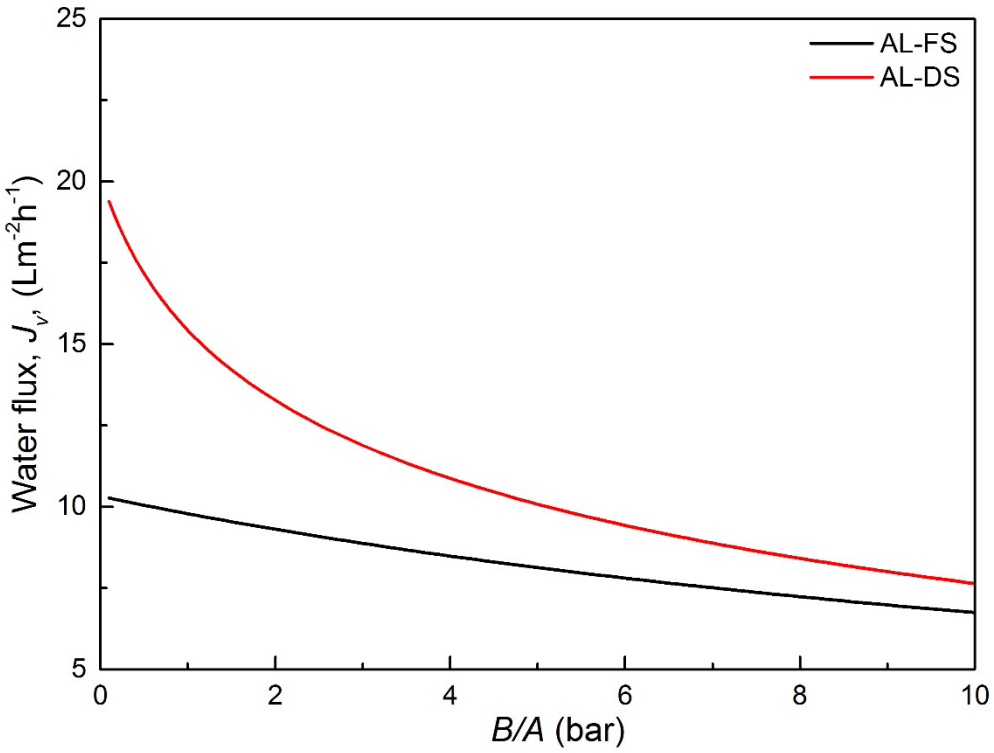

Figure G1. The simulated relationship between *B/A* and FO water flux J_v at specific conditions. Simulation conditions: the K_m was set at 4.6 Lm^{-2}h^{-1} based on the calculation of experimental results, π_{draw} and π_{feed} were fixed at 48.9 and 0.49 bar (i.e., the osmotic pressure of 1 M NaCl and 10 mM NaCl, respectively), and *A* was fixed at 2.21 Lm^{-2}h^{-1}bar^{-1} (i.e., the water permeability of the control membrane).

According to Wei et al. [43], increased reverse solute diffusion can promote more severe internal concentration polarization: draw solutes diffused through the rejection layer would accumulate inside the porous support layer, leading to a loss of effective osmotic driving force. This effect is reflected by the *B/A* term in the classical internal concentration polarization equations for FO membranes [34]:

$$J_v = K_m \left[ln \frac{\pi_{draw}+B/A}{\pi_{feed}+B/A+J_v/A} \right] \quad \text{(AL-FS)} \qquad \text{(G1)}$$

$$J_v = K_m \left[ln \frac{\pi_{draw}+B/A-J_v/A}{\pi_{feed}+B/A} \right] \quad \text{(AL-DS)} \qquad \text{(G2)}$$

where J_v is the FO water flux, K_m is the mass transfer coefficient related the properties of

support layer, π_{draw} and π_{feed} are the osmotic pressure of the draw and feed solutions, respectively. *A* and *B* are the water permeability and solute permeability coefficients, respectively, and the ratio *B/A* represents the membrane selectivity. According to Eqs. (G1) and (G2), reducing *B/A*, i.e., improving membrane selectivity, can effectively increase FO water flux (Figure G1).

References

[1] T.Y. Cath, A.E. Childress, M. Elimelech, Forward osmosis: principles, applications, and recent developments, J. Membr. Sci., 281 (2006) 70-87.

[2] S. Zhao, L. Zou, C.Y. Tang, D. Mulcahy, Recent developments in forward osmosis: opportunities and challenges, J. Membr. Sci., 396 (2012) 1-21.

[3] J.R. McCutcheon, R.L. McGinnis, M. Elimelech, Desalination by ammonia–carbon dioxide forward osmosis: influence of draw and feed solution concentrations on process performance, J. Membr. Sci., 278 (2006) 114-123.

[4] J.R. McCutcheon, R.L. McGinnis, M. Elimelech, A novel ammonia—carbon dioxide forward (direct) osmosis desalination process, Desalination, 174 (2005) 1-11.

[5] J. Zhang, Q. She, V.W.C. Chang, C.Y. Tang, R.D. Webster, Mining nutrients (N, K, P) from urban source-separated urine by forward osmosis dewatering, Environ. Sci. Technol., 48 (2014) 3386-3394.

[6] Y. Cui, Q. Ge, X.-Y. Liu, T.-S. Chung, Novel forward osmosis process to effectively remove heavy metal ions, J. Membr. Sci., 467 (2014) 188-194.

[7] K. Lutchmiah, A.R.D. Verliefde, K. Roest, L.C. Rietveld, E.R. Cornelissen, Forward osmosis for application in wastewater treatment: a review, Water Res., 58 (2014) 179-197.

[8] K.L. Lee, R.W. Baker, H.K. Lonsdale, Membranes for power generation by pressure-retarded osmosis, J. Membr. Sci., 8 (1981) 141-171.

[9] A. Achilli, T.Y. Cath, A.E. Childress, Power generation with pressure retarded osmosis: An experimental and theoretical investigation, J. Membr. Sci., 343 (2009) 42-52.

[10] Q. She, X. Jin, C.Y. Tang, Osmotic power production from salinity gradient resource by pressure retarded osmosis: effects of operating conditions and reverse solute diffusion, J. Membr. Sci., 401 (2012) 262-273.

[11] B. Mi, M. Elimelech, Chemical and physical aspects of organic fouling of forward osmosis membranes, J. Membr. Sci., 320 (2008) 292-302.

[12] E.R. Cornelissen, D. Harmsen, K.F. De Korte, C.J. Ruiken, J.-J. Qin, H. Oo, L.P. Wessels, Membrane fouling and process performance of forward osmosis membranes on activated sludge, J. Membr. Sci., 319 (2008) 158-168.

[13] Y. Gu, Y.-N. Wang, J. Wei, C.Y. Tang, Organic fouling of thin-film composite polyamide and cellulose triacetate forward osmosis membranes by oppositely charged macromolecules, Water Res., 47 (2013) 1867-1874.

[14] Z.-Y. Li, V. Yangali-Quintanilla, R. Valladares-Linares, Q. Li, T. Zhan, G. Amy, Flux patterns and membrane fouling propensity during desalination of seawater by forward osmosis, Water Res., 46 (2012) 195-204.

[15] J.R. McCutcheon, M. Elimelech, Influence of concentrative and dilutive internal concentration polarization on flux behavior in forward osmosis, J. Membr. Sci., 284 (2006) 237-247.

[16] R.W. Field, J.J. Wu, Mass transfer limitations in forward osmosis: Are some potential applications overhyped?, Desalination, 318 (2013) 118-124.

[17] D. Rana, T. Matsuura, Surface modifications for antifouling membranes, Chem. Rev., 110 (2010) 2448-2471.

[18] A. Tiraferri, Y. Kang, E.P. Giannelis, M. Elimelech, Superhydrophilic thin-film composite forward osmosis membranes for organic fouling control: fouling behavior and antifouling mechanisms, Environ. Sci. Technol., 46 (2012) 11135-11144.
[19] H.-L. Yang, J. Chun-Te Lin, C. Huang, Application of nanosilver surface modification to RO membrane and spacer for mitigating biofouling in seawater desalination, Water Res., 43 (2009) 3777-3786.
[20] B.D. McCloskey, H.B. Park, H. Ju, B.W. Rowe, D.J. Miller, B.J. Chun, K. Kin, B.D. Freeman, Influence of polydopamine deposition conditions on pure water flux and foulant adhesion resistance of reverse osmosis, ultrafiltration, and microfiltration membranes, Polymer, 51 (2010) 3472-3485.
[21] D.J. Miller, P.A. Araujo, P.B. Correia, M.M. Ramsey, J.C. Kruithof, M.C.M. van Loosdrecht, B.D. Freeman, D.R. Paul, M. Whiteley, J.S. Vrouwenvelder, Short-term adhesion and long-term biofouling testing of polydopamine and poly (ethylene glycol) surface modifications of membranes and feed spacers for biofouling control, Water Res., 46 (2012) 3737-3753.
[22] J. Jiang, L. Zhu, L. Zhu, H. Zhang, B. Zhu, Y. Xu, Antifouling and antimicrobial polymer membranes based on bioinspired polydopamine and strong hydrogen-bonded poly (N-vinyl pyrrolidone), ACS Appl. Mater. Interfaces, 5 (2013) 12895-12904.
[23] K.-Y. Kim, E. Yang, M.-Y. Lee, K.-J. Chae, C.-M. Kim, I.S. Kim, Polydopamine coating effects on ultrafiltration membrane to enhance power density and mitigate biofouling of ultrafiltration microbial fuel cells (UF-MFCs), Water Res., 54 (2014) 62-68.
[24] H. Lee, S.M. Dellatore, W.M. Miller, P.B. Messersmith, Mussel-inspired surface chemistry for multifunctional coatings, Science, 318 (2007) 426-430.
[25] B.D. McCloskey, Novel surface modifications and materials for fouling resistant water purification membranes, in, University of Texas at Austin, 2009.
[26] H. Guo, Y. Deng, Z. Tao, Z. Yao, J. Wang, C. Lin, T. Zhang, B. Zhu, C.Y. Tang, Does Hydrophilic Polydopamine Coating Enhance Membrane Rejection of Hydrophobic Endocrine-Disrupting Compounds?, Environ. Sci. Technol. Lett., 3 (2016) 332-338.
[27] S. Kasemset, A. Lee, D.J. Miller, B.D. Freeman, M.M. Sharma, Effect of polydopamine deposition conditions on fouling resistance, physical properties, and permeation properties of reverse osmosis membranes in oil/water separation, J. Membr. Sci., 425 (2013) 208-216.
[28] H.-C. Yang, J. Luo, Y. Lv, P. Shen, Z.-K. Xu, Surface engineering of polymer membranes via mussel-inspired chemistry, J. Membr. Sci., 483 (2015) 42-59.
[29] J.T. Arena, B. McCloskey, B.D. Freeman, J.R. McCutcheon, Surface modification of thin film composite membrane support layers with polydopamine: enabling use of reverse osmosis membranes in pressure retarded osmosis, J. Membr. Sci., 375 (2011) 55-62.
[30] J.T. Arena, S.S. Manickam, K.K. Reimund, B.D. Freeman, J.R. McCutcheon, Solute and water transport in forward osmosis using polydopamine modified thin film composite membranes, Desalination, 343 (2014) 8-16.
[31] G. Han, S. Zhang, X. Li, N. Widjojo, T.-S. Chung, Thin film composite forward osmosis membranes based on polydopamine modified polysulfone substrates with enhancements in both water flux and salt rejection, Chem. Eng. Sci., 80 (2012) 219-231.
[32] H. Guo, Y. Deng, Z. Yao, Z. Yang, J. Wang, C. Lin, T. Zhang, B. Zhu, C.Y. Tang, A

498 highly selective surface coating for enhanced membrane rejection of endocrine disrupting
499 compounds: Mechanistic insights and implications, Water Res., (2017).
500 [33] J. Ren, J.R. McCutcheon, A new commercial thin film composite membrane for forward
501 osmosis, Desalination, 343 (2014) 187-193.
502 [34] C.Y. Tang, Q. She, W.C.L. Lay, R. Wang, A.G. Fane, Coupled effects of internal
503 concentration polarization and fouling on flux behavior of forward osmosis membranes
504 during humic acid filtration, J. Membr. Sci., 354 (2010) 123-133.
505 [35] X. Jin, Q. She, X. Ang, C.Y. Tang, Removal of boron and arsenic by forward osmosis
506 membrane: influence of membrane orientation and organic fouling, J. Membr. Sci., 389 (2012)
507 182-187.
508 [36] S.H. Kim, S.-Y. Kwak, T. Suzuki, Positron annihilation spectroscopic evidence to
509 demonstrate the flux-enhancement mechanism in morphology-controlled thin-film-composite
510 (TFC) membrane, Environ. Sci. Technol., 39 (2005) 1764-1770.
511 [37] C.Y. Tang, Y.-N. Kwon, J.O. Leckie, Probing the nano-and micro-scales of reverse
512 osmosis membranes—a comprehensive characterization of physiochemical properties of
513 uncoated and coated membranes by XPS, TEM, ATR-FTIR, and streaming potential
514 measurements, J. Membr. Sci., 287 (2007) 146-156.
515 [38] E.M. Vrijenhoek, S. Hong, M. Elimelech, Influence of membrane surface properties on
516 initial rate of colloidal fouling of reverse osmosis and nanofiltration membranes, J. Membr.
517 Sci., 188 (2001) 115-128.
518 [39] D. Xiao, C.Y. Tang, J. Zhang, W.C.L. Lay, R. Wang, A.G. Fane, Modeling salt
519 accumulation in osmotic membrane bioreactors: implications for FO membrane selection and
520 system operation, J. Membr. Sci., 366 (2011) 314-324.
521 [40] S. Zou, Y. Gu, D. Xiao, C.Y. Tang, The role of physical and chemical parameters on
522 forward osmosis membrane fouling during algae separation, J. Membr. Sci., 366 (2011)
523 356-362.
524 [41] Y. Zhao, A. Vararattanavech, X. Li, C. HélixNielsen, T. Vissing, J. Torres, R. Wang, A.G.
525 Fane, C.Y. Tang, Effects of proteoliposome composition and draw solution types on
526 separation performance of aquaporin-based proteoliposomes: implications for seawater
527 desalination using aquaporin-based biomimetic membranes, Environ. Sci. Technol., 47 (2013)
528 1496-1503.
529 [42] Q. Saren, C.Q. Qiu, C.Y. Tang, Synthesis and characterization of novel forward osmosis
530 membranes based on layer-by-layer assembly, Environ. Sci. Technol., 45 (2011) 5201-5208.
531 [43] J. Wei, C. Qiu, Y.-N. Wang, R. Wang, C.Y. Tang, Comparison of NF-like and RO-like
532 thin film composite osmotically-driven membranes—implications for membrane selection
533 and process optimization, J. Membr. Sci., 427 (2013) 460-471.
534 [44] D. Chen, J.R. Werber, X. Zhao, M. Elimelech, A facile method to quantify the carboxyl
535 group areal density in the active layer of polyamide thin-film composite membranes, J.
536 Membr. Sci., 534 (2017) 100-108.
537 [45] B.D. McCloskey, H.B. Park, H. Ju, B.W. Rowe, D.J. Miller, B.D. Freeman, A bioinspired
538 fouling-resistant surface modification for water purification membranes, J. Membr. Sci., 413
539 (2012) 82-90.
540 [46] H. Karkhanechi, R. Takagi, H. Matsuyama, Biofouling resistance of reverse osmosis

membrane modified with polydopamine, Desalination, 336 (2014) 87-96.
[47] F. Li, J. Meng, J. Ye, B. Yang, Q. Tian, C. Deng, Surface modification of PES ultrafiltration membrane by polydopamine coating and poly (ethylene glycol) grafting: morphology, stability, and anti-fouling, Desalination, 344 (2014) 422-430.
[48] P. Xu, C. Bellona, J.E. Drewes, Fouling of nanofiltration and reverse osmosis membranes during municipal wastewater reclamation: membrane autopsy results from pilot-scale investigations, J. Membr. Sci., 353 (2010) 111-121.
[49] Q. She, R. Wang, A.G. Fane, C.Y. Tang, Membrane fouling in osmotically driven membrane processes: a review, J. Membr. Sci., 499 (2016) 201-233.
[50] F. Meng, S.-R. Chae, A. Drews, M. Kraume, H.-S. Shin, F. Yang, Recent advances in membrane bioreactors (MBRs): membrane fouling and membrane material, Water Res., 43 (2009) 1489-1512.
[51] W.K. Cho, B. Kong, I.S. Choi, Highly efficient non-biofouling coating of zwitterionic polymers: poly ((3-(methacryloylamino) propyl)-dimethyl (3-sulfopropyl) ammonium hydroxide), Langmuir, 23 (2007) 5678-5682.
[52] C. Liu, J. Lee, J. Ma, M. Elimelech, Antifouling Thin-Film Composite Membranes by Controlled Architecture of Zwitterionic Polymer Brush Layer, Environ. Sci. Technol., 51 (2017) 2161-2169.
[53] G. Liu, W. Jin, N. Xu, Graphene-based membranes, Chem. Soc. Rev., 44 (2015) 5016-5030.
[54] E. Yang, C.-M. Kim, J.-h. Song, H. Ki, M.-H. Ham, I.S. Kim, Enhanced desalination performance of forward osmosis membranes based on reduced graphene oxide laminates coated with hydrophilic polydopamine, Carbon, 117 (2017) 293-300.
[55] Z. Yang, Y. Wu, J. Wang, B. Cao, C.Y. Tang, In Situ Reduction of Silver by Polydopamine: A Novel Antimicrobial Modification of a Thin-Film Composite Polyamide Membrane, Environ. Sci. Technol., 50 (2016) 9543-9550.
[56] C. Liu, A.F. de Faria, J. Ma, M. Elimelech, Mitigation of Biofilm Development on Thin-Film Composite Membranes Functionalized with Zwitterionic Polymers and Silver Nanoparticles, Environ. Sci. Technol., (2017).